Full Poincaré sphere coverage with plasmonic nanoslit metamaterials at Fano resonance

M. R. Shcherbakov,[1] M. I. Dobynde,[1] T. V. Dolgova,[1] D.-P. Tsai,[2,3] and A. A. Fedyanin[1,*]
[1]*Faculty of Physics, Lomonosov Moscow State University, Moscow 119991, Russia*
[2]*Department of Physics, National Taiwan University, Taipei 10617, Taiwan*
[3]*Research Center for Applied Sciences, Academia Sinica, Taipei 11529, Taiwan*
(Received 4 October 2010; published 3 November 2010)

A form-birefringent plasmonic metamaterial of the subwavelength thickness is used to convert the light's polarization state in a way to cover the whole Poincaré sphere's surface by adjusting the experimental configuration. This optical anisotropy is induced by grating surface plasmon polaritons of a nanoslit array made in a thin golden film with the narrow spectral Fano resonance. Phase delay between linearly polarized states introduced by the sample reaches the value of 0.85π in the visible corresponding to the effective ordinary-extraordinary refractive index difference of $\Delta n \simeq 10.4$.

DOI: 10.1103/PhysRevB.82.193402 PACS number(s): 73.20.Mf, 77.22.Ej, 78.20.Fm, 78.67.Pt

Thin metallic films shaped at the nanoscale have become of exceptional interest due to their electromagnetic response being highly dependent on the pattern configuration which allows one to pre-engineer their optical properties. Extraordinary optical transmission[1] media, negative refractive index metamaterials,[2] and artificially anisotropic[3,4] and chiral[5,6] metamaterials are the few examples of plasmonic objects acquiring their unusual optical properties through nanostructuring. Optical response of such materials is often defined by the excitation of propagating surface plasmon polaritons (SPPs) which are coupled onto the metallic surface through the periodicity of the structure itself.[7,8] In some cases, these excitations give rise to sharp Fano-type spectral lines[9–11] which have been recently intensively used for manipulation of transmittance of the nanostructured metal films from almost perfect[12,13] to suppressed transmission.[14]

Controlling the polarization state of transmitted or reflected light with anisotropic plasmonic nanostructures has been studied for a long time[15] and contemporary results in this area include giant specific linear birefringence and dichroism[16–20] in the spectral vicinity of plasmonic resonances. However, high phase delays between ordinary and extraordinary waves could not be achieved with broad spectral lines of about 100 nm full width at half maximum used in preceding works for the reasons given in the discussion section of this paper.

In this Brief Report we show how a narrow Fano resonance in a plasmonic metamaterial could be utilized to induce huge phase delay between transmitted linearly polarized eigenstates. It is demonstrated that the resulting birefringence can be controlled by varying the angle of incidence in the range of only 8° from $\Delta n=4.4$ to $\Delta n=10.4$, where Δn is the difference between effective refractive indices of ordinary and extraordinary waves. It is shown that the polarization state of the light output from a system with a Fano resonance could cover the whole Poincaré sphere which was unattainable with previously concerned structured films of subwavelength thicknesses.

A system which optical response consists of a coherent superposition of Lorentz-resonance response and background signal would possess a spectral line shape called Fano resonance.[21] The general expression for the complex transfer function of a Fano-resonance system can be written as follows:

$$T(\omega) = A + \frac{Be^{\imath\phi}}{\omega - \omega_0 + \imath\gamma},$$

where A and B are the amplitudes of background and resonant signals, ϕ is the relative phase between them, ω_0 is the resonant frequency, and γ is the damping constant. Consider a medium with the following Jones' representation:[22]

$$J(\omega) \propto \begin{pmatrix} T(\omega) & 0 \\ 0 & T_0 \end{pmatrix},$$

where T_0 is real. Here, $T(\omega)$ and T_0 are the field transmission coefficients for the E_x and E_y components of the incident E field, respectively. The modeled spectra of $|T(\omega)|^2$ and $\varphi(\omega) \equiv \arg[T(\omega)]$ obtained with the following parameters: $A=0.14$, $B=2\times10^{13}$ s^{-1}, $\phi=-0.2\pi$, $\omega_0=2.7\times10^{15}$ s^{-1} ($\lambda \simeq 700$ nm), and $\gamma=5\times10^{13}$ s^{-1} ($\Delta\lambda \simeq 15$ nm) are shown in Fig. 1(a). The phase spectrum demonstrates the phase delay up to π between orthogonal linear polarizations, i.e., linear birefringence. Suppose that the incident polarization state is $\mathbf{P}_{in}=(1,0)$ (x polarized) and the system's optical axis is oriented at an angle ψ with respect to the Oy axis. The Jones' matrix of such a birefringent medium is written as follows:[22]

$$J(\omega) \propto \begin{pmatrix} \sin^2\psi + \xi e^{\imath\varphi}\cos^2\psi & \sin\psi\cos\psi(1-\xi e^{\imath\varphi}) \\ \sin\psi\cos\psi(1-\xi e^{\imath\varphi}) & \cos^2\psi + \xi e^{\imath\varphi}\sin^2\psi \end{pmatrix},$$

where $\xi \equiv |T(\omega)|/T_0$. The output state is then written as a function of ψ

$$\mathbf{P}_{out}(\psi) \propto \begin{pmatrix} \sin^2\psi + \xi e^{\imath\varphi}\cos^2\psi \\ \sin\psi\cos\psi(1-\xi e^{\imath\varphi}) \end{pmatrix}.$$

Figure 1(b) shows the map of the output polarization states put onto the surface of the Poincaré sphere. The parameters of the Fano resonance were chosen in such a way that as a result of linear birefringence and dichroism the output polarization states cover the whole Poincaré sphere's surface by varying the azimuthal angle ψ and the radiation wavelength λ. Curves shown in Fig. 1(b) represent the sets of output states at eight particular wavelengths in the range of λ

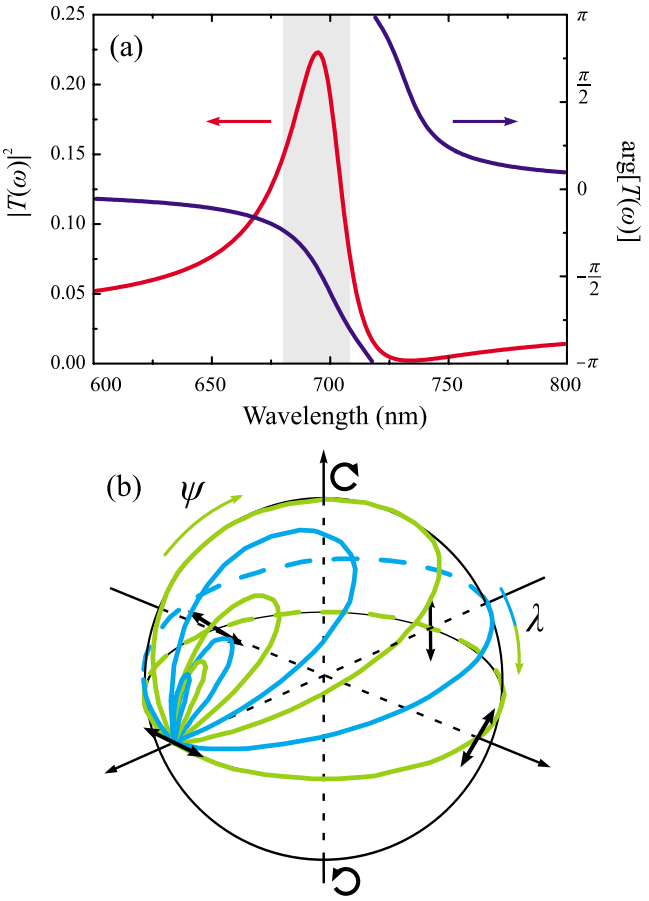

FIG. 1. (Color online) (a) Transfer function $|T(\omega)|^2$ and phase spectra of a system with a Fano resonance. (b) The Poincaré sphere representing the map of polarization transformations done by the system under study. The input state is (1,0) in Jones' representation. Each curve describes a set of output states for azimuthal angle ψ varying from 0° to 90°. Different curves stand for different wavelengths in the vicinity of Fano resonance from the gray area in panel (a). Although not indicated, the bottom hemisphere is covered in the same way with $-\psi$ angles due to symmetry relations.

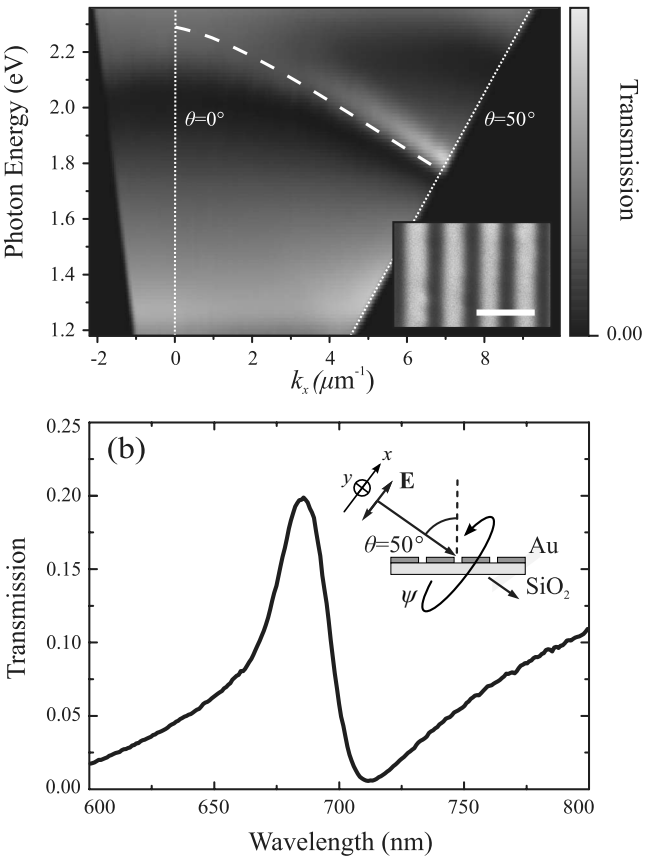

FIG. 2. (a) Transmission coefficient of the nanoslit sample as a function of photon energy and transversal wave number of the incident p-polarized light. SPP excited with the blazing minus-first diffraction order is present. The dispersion relation of SPP propagating at gold-fused silica interface estimated using expression (1) is denoted with white dashed line. The inset shows the scanning electron microscopy picture of the sample, the bar equals to 500 nm. (b) The transmission spectrum at the 50° incidence indicating a Fano-type resonance for the p-polarized light.

=680–710 nm for the ease of comprehension. Continuous variation in the wavelength gives one an access to every state on the Poincaré sphere. Since there are five independent parameters, A, B, ω, γ, and φ, controlling the polarization properties of the concerned system, the full analytical study of the parameter range which allows the full Poincaré sphere coverage is complicated. Nevertheless, the parameters presented here are realistic and sufficient to demonstrate the principal possibility of the full coverage.

Optical response of nanoslit arrays in thin golden film was studied to experimentally observe the coverage of Poincaré sphere. The sample of nanoslit plasmonic metamaterial was fabricated by the electron-beam lithography technique with the negative resist. After the lift-off process the grating period was a_0=310 nm with the width of the slits being approximately 80 nm and golden film thickness of 30 nm. Total area of the nanostructured film was 300×300 μm^2. Transmission spectra were carried out using the white-light microspectroscopy setup with the spectral range of λ =400–800 nm, spectral accuracy of 0.8 nm, the focal spot of ~200 μm in diameter, and the numerical aperture of the focusing system of 0.04. The input and output polarization states were controlled by two broadband Glan-Taylor prism polarizers. Since analyzing the light's state with a polarizer does not provide one with the information about the E-field rotation direction and depolarization, an achromatic quarter-wave plate was used before the analyzer to acquire the lacking Stokes' parameters. The details of the phase delay acquisition method could be found in preceding papers.[20]

The transmission of the nanoslit sample is presented in Fig. 2(a) as a function of incident light's photon energy and wave-vector projection onto a sample's plane k_x for the p-polarized light $\mathbf{e}_x$=(1,0). Sharp and angle-dependent Fano-type resonance is observed in the visible range; a cross section of the transmission function at the angle of incidence θ=50° is shown in Fig. 2(b). The origin of the Fano-type optical response lies in the coherent superposition of the grating SPPs resonance response and the background signal directly transmitted through the 30-nm-thick golden film.[7] The central wavelength of SPP resonance which is not generally situated neither in the maximum nor in the minimum

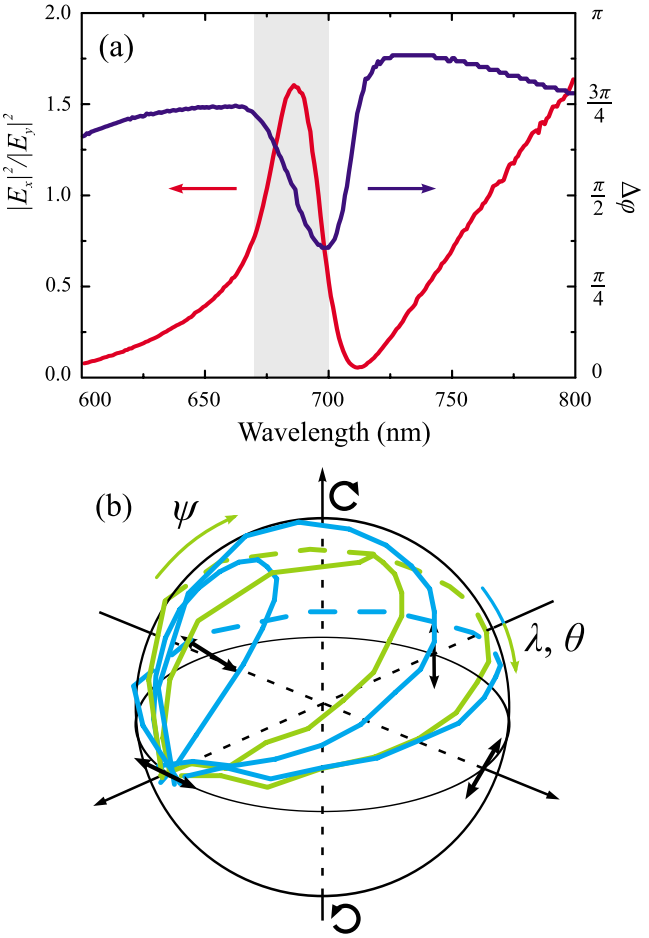

FIG. 3. (Color online) (a) Linear birefringence and dichroism of the nanoslit sample represented by the phase retardation $\Delta\varphi$ and $|E_x|^2/|E_y|^2$ spectra, respectively, measured at the 50° incidence. (b) The Poincaré sphere representing the map of experimental polarization transformations done by the system under study. The input state is (1,0). Each curve describes a set of output states for azimuthal angle ψ varying from 0° to 90°. Different curves stand for different wavelengths in the vicinity of Fano resonance or different angles of incidence, calculated using the $\partial\theta/\partial\lambda$ expression from the main text. Although not indicated, the bottom hemisphere is covered in the same way with $-\psi$ angles due to symmetry relations.

of the transmission spectrum could be estimated using the expression carried out from the phase-matching condition[8]

$$\lambda_{SPP} = a_0\left(\sqrt{\frac{\varepsilon_{Au}\varepsilon_{SiO_2}}{\varepsilon_{Au}+\varepsilon_{SiO_2}}} + \sin\theta\right), \qquad (1)$$

where ε_{Au} and ε_{SiO_2} are dielectric permittivities of gold and fused silica, respectively, and represented in Fig. 2(a) with the dashed white line. The phase delay $\Delta\varphi$ between E_y and E_x output E-field's components and dichroism $|E_x|^2/|E_y|^2$ are measured in the spectral domain and shown in Fig. 3(a) for $\theta=50°$. The phase difference varies from 0.38π to 0.85π which could be obtained by a medium of the same thickness with extreme ordinary-extraordinary refractive indices differences of $\Delta n \simeq 4.4-10.4$.

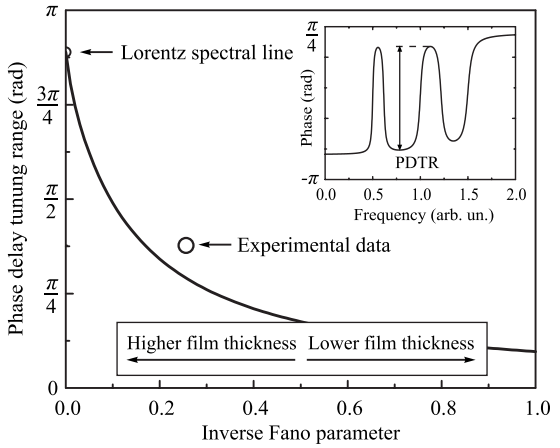

FIG. 4. The PDTR as a function of the inverse Fano parameter of the three-Fano-resonance system. The value of the PDTR is defined as the maximum phase drop near the middle resonance as depicted on the phase spectrum in the inset. The tuning is achieved by changing the angle of incidence therefore shifting the resonances in the spectral domain. The open dot denotes the experimentally achieved PDTR of 0.38π in the vicinity of plasmonic resonance with $1/F=0.26$.

The map of polarization conversions produced by the sample is presented on the upper hemisphere of the Poincaré sphere in Fig. 3(b) for spectral region of $\lambda=670-700$ nm and for the azimuthal angle interval of $\psi=0°-90°$. The variation in the azimuthal angle ψ is performed in this representation by rotating the sample around the k vector of the incident light rather than by changing the polarization itself. Keeping the incident light's polarization state always fixed to be $\mathbf{e}_x=(1,0)$ leads to the curves on the Poincaré sphere forming closed loops. The depolarization of the output state was always below the experimental uncertainty (<0.003 in ellipticity terms). Nevertheless more experimental data are available, the data are represented by curves at only five particular wavelengths in the corresponding wavelength range for better visualization. The intermediate polarization states are covered by varying the wavelength at smaller steps.

A notable feature of the plasmonic system is that its polarization properties could be also tuned at the fixed wavelength by changing the angle of incidence θ. This ability allows one to cover the remarkable part of the Poincaré sphere by varying θ in the narrow range of values. Using the dispersion relation in Eq. (1) and assuming the wavelength independence of the material constants the angle range equivalent to the wavelength range of 670–700 nm is estimated from the expression $\partial\theta/\partial\lambda=(a_0\sin\theta)^{-1}$ to be $\theta \in [46°, 54°]$. This angle-controlled tunability differs from angular properties of conventional polarization optical elements. The metamaterial under study also differs qualitatively from the commonly used broadband wire-grid polarizers[23] and form-birefringent dielectric[24] and metallic[3] gratings since the latter are operating in the nonresonant regime which does not allow high angular dispersion values.

Nevertheless the experimental realization of the Poincaré sphere coverage provided here does not involve all the possible output polarization states, the performance of the plas-

monic nanoslit array could be improved. So-called Fano parameter $F=B/(A\gamma)$ is one of the key parameters defining the polarization properties of the system and it stands for the relation between the resonant and background contributions comprising the Fano-type response. To demonstrate the effect of the background and resonant terms ratio on the polarization transformation abilities of the structure we modeled the response of three Fano resonances equidistantly distributed in spectral domain $(\omega_1=\omega_2/2=\omega_3/3=0.5)$ which is a commonplace for systems with grating plasmon resonances. The resonances possess the same Fano parameter. The inset in Fig. 4 shows the phase spectra of the resonances indicating the phase retardations achievable in the site of the middle resonance. The phase retardation tuned by changing the wavelength or the angle of incidence makes up the phase delay tuning range (PDTR) which is depicted in the inset in Fig. 4 as the maximum drop of the phase near the middle resonance. It is seen that PDTR is decreased with the increase in the width of the resonances and this is the reason why the narrowness of the resonances is crucial at this point. Figure 4 shows the calculated dependence of the PDTR on the inverse Fano parameter $1/F$. It is seen that Lorentzian spectral line is more appropriate for attaining the highest PDTR. The nanoslit sample studied delivers 0.38π of PDTR which could be increased by, e.g., increasing the thickness of the film and attenuating the background contribution. On the other hand, the Lorentz shape is achieved on thick films only which implies unwanted low transmittance. Thus, the thickness of the metallic film should be the key parameter to optimize when designing the artificial birefringence of nanoslit metamaterials.

In conclusion, it is shown how an artificial birefringent medium with a narrow Fano-type spectral line could be used to transform light's polarization from initial state to an arbitrary state by choosing the configuration of the experiment. Experimental realization of such a polarization converter is provided with plasmonic arrays of nanoslits in a thin golden film showing enormous specific birefringence and dichroism in the vicinity of the SPP resonance. Considerable part of the unit Poincaré sphere's surface is shown to be attainable with the sample. The way of optimizing the performance of the sample by varying the Fano parameter of the resonance controlled by the thickness of the sample is proposed. Established data allow one to expect the improvement of the results by use of finer samples and by numerical modeling giving a chance for nanoslit metamaterials to be a promising candidate for future optoelectronic devices.

This work was supported by Russian Foundation of Basic Research and Ministry of Education and Science (Russia) under Grants No. P1465, No. P946, No. 02.740.11.0561 and by grants of National Science Council (Taiwan) under Grants No. NSC-96-2923-M-002-002-MY3 and No. NSC-99-2120-M-002-012.

*fedyanin@nanolab.phys.msu.ru

[1] T. W. Ebbesen, H. J. Lezec, H. F. Ghaemi, T. Thio, and P. A. Wolff, Nature (London) **391**, 667 (1998).
[2] V. M. Shalaev, Nat. Photonics **1**, 41 (2007).
[3] B. Schnabel, E. B. Kley, and F. Wyrowski, Opt. Eng. **38**, 220 (1999).
[4] R. Gordon, A. G. Brolo, A. McKinnon, A. Rajora, B. Leathem, and K. L. Kavanagh, Phys. Rev. Lett. **92**, 037401 (2004).
[5] E. Plum, V. A. Fedotov, A. S. Schwanecke, N. I. Zheludev, and Y. Chen, Appl. Phys. Lett. **90**, 223113 (2007).
[6] M. Decker, M. W. Klein, M. Wegener, and S. Linden, Opt. Lett. **32**, 856 (2007).
[7] U. Fano, J. Opt. Soc. Am. **31**, 213 (1941).
[8] H. Raether, *Surface-Plasmons on Smooth and Rough Surfaces and on Gratings* (Springer, Berlin, 1988).
[9] M. Sarrazin, J.-P. Vigneron, and J.-M. Vigoureux, Phys. Rev. B **67**, 085415 (2003).
[10] C. Genet, M. P. van Exter, and J. P. Woerdman, Opt. Commun. **225**, 331 (2003).
[11] C. Billaudeau, S. Collin, F. Pardo, N. Bardou, and J.-L. Pelouard, Opt. Express **17**, 3490 (2009).
[12] J. A. Porto, F. J. Garcia-Vidal, and J. B. Pendry, Phys. Rev. Lett. **83**, 2845 (1999).
[13] S. Collin, G. Vincent, R. Haidar, N. Bardou, S. Rommeluere, and J.-L. Pelouard, Phys. Rev. Lett. **104**, 027401 (2010).
[14] J. Braun, B. Gompf, G. Kobiela, and M. Dressel, Phys. Rev. Lett. **103**, 203901 (2009).
[15] G. P. Bryan-Brown, J. R. Sambles, and M. C. Hutley, J. Mod. Opt. **37**, 1227 (1990).
[16] D. Heitmann, Opt. Commun. **20**, 292 (1977).
[17] A. Drezet, C. Genet, and T. W. Ebbesen, Phys. Rev. Lett. **101**, 043902 (2008).
[18] S.-Y. Hsu, K.-L. Lee, E.-H. Lin, M.-C. Lee, and P.-K. Wei, Appl. Phys. Lett. **95**, 013105 (2009).
[19] J. Sung, M. Sukharev, E. M. Hicks, R. P. Van Duyne, T. Seideman, and K. G. Spears, J. Phys. Chem. C **112**, 3252 (2008).
[20] M. R. Shcherbakov, P. P. Vabishchevich, M. I. Dobynde, T. V. Dolgova, A. S. Sigov, C. M. Wang, D. P. Tsai, and A. A. Fedyanin, JETP Lett. **90**, 433 (2009).
[21] U. Fano, Phys. Rev. **124**, 1866 (1961).
[22] A. Gerald and J. M. Burch, *Introduction to Matrix Methods in Optics* (Wiley, New York, 1975).
[23] P. K. Cheo and C. D. Bass, Appl. Phys. Lett. **18**, 565 (1971).
[24] D. C. Flanders, Appl. Phys. Lett. **42**, 492 (1983).